Dynamic changes in myelin aberrations and oligodendrocyte generation in chronic amyloidosis in mice and men.

Dynamic changes in myelin aberrations and oligodendrocyte generation in chronic amyloidosis in mice and men.

Behrendt G, Baer K, Buffo A, Curtis MA, Faull RL, Rees MI, Götz M, Dimou L.

Glia. 2013 Feb;61(2):273-86. doi: 10.1002/glia.22432.

Dynamic changes in myelin aberrations and oligodendrocyte generation in chronic amyloidosis in mice and men

Journal:	*GLIA*
Manuscript ID:	GLIA-00192-2012.R1
Wiley - Manuscript type:	Original Research Article
Date Submitted by the Author:	08-Sep-2012

Complete List of Authors:	Behrendt, Gwendolyn; LMU Munich, Physiological Genomics Baer, Kristin; college of medicine, Institute of Life science Buffo, Annalisa; University of Turin, Department of Neuroscience Neuroscience Institute Cavalieri Ottolenghi (NICO) Curtis, Maurice; Auckland University, Anatomy with Radiology; Faull, Richard; University of Auckland, Anatomy with Radiology, School of Medical Sciences Rees, Mark; college of medicine, Institute of Life science Götz, Magdalena; HelmholtzZentrum, Institute of stem cell research Dimou, Leda; LMU Munich, Physiological Genomics

Key Words:	OPCs, NG2, Alzheimer`s disease, proliferation, amyloidosis

Dynamic changes in myelin aberrations and oligodendrocyte generation in chronic amyloidosis in mice and men

Gwendolyn Behrendt [1], Kristin Baer [3], Annalisa Buffo [4], Maurice A. Curtis [5], Richard L. Faull [5], Mark I. Rees [3], Magdalena Götz [1,2] and Leda Dimou [1,2,*]

[1]Physiological Genomics, Institute of Physiology, Ludwig-Maximilians University Munich, Germany; [2]Institute for Stem Cell Research, HelmholtzZentrum, Neuherberg, Germany; [3]Institute of Life Science College of Medicine, University, Swansea, UK; [4]Department of Neuroscience, Neuroscience Institute Cavalieri Ottolenghi (NICO), University of Turin, Italy; [5]Department of Anatomy with Radiology and Centre for Brain Research, Faculty of Medical and Health Science, University of Auckland, New Zealand; * Corresponding author

Corresponding author:

Leda Dimou

Physiological Genomics

Ludwig-Maximilians University

80336 Munich

Germany

Phone: +49-89-2180 75527

Fax: +49-89-2180 75216

leda.dimou@lrz.uni-muenchen.de

Running title: Oligodendrocyte repair in APPPS1 mice

Number of words for Abstract: 238, for Introduction: 548, for Material and Methods: 1103, for Results: 1897, for Discussion: 1409, for Acknowledgements: 122, for References: 1824, for Tables: 390 and for Figure legends: 788

Total number of words: 8328

Number of figures: 6

Supplemental figures: 2

Tables: 3

Key words: OPCs, NG2, proliferation, amyloidosis, Alzheimer's Disease

Abstract

Myelin loss is frequently observed in human Alzheimer's disease (AD) and may constitute to AD-related cognitive decline. A potential source to repair myelin defects are the oligodendrocyte progenitor cells (OPCs) present in the adult brain. However, until now little is known about the reaction of these cells toward amyloid plaque deposition neither in human AD patients nor in the appropriate mouse models. Therefore, we analyzed cells of the oligodendrocyte lineage in a mouse model with chronic plaque deposition (APPPS1 mice) and samples from human patients.

In APPPS1 mice defects in myelin integrity and myelin amount were prevalent at 6 months of age but normalized to control levels in 9 months old mice. Concomitantly, we observed an increase in the proliferation and differentiation of OPCs in the APPPS1 mice at this specific time window (6-8 months) implying that improvements in myelin aberrations may result from repair mechanisms mediated by OPCs.

However, while we observed a higher number of cells of the oligodendrocyte lineage (Olig2+ cells) in APPPS1 mice, OLIG2+ cells were decreased in number in *post-mortem* human AD cortex. Our data demonstrate that oligodendrocyte progenitors specifically react to amyloid plaque deposition in an AD-related mouse model as well as in human AD pathology, although with distinct outcomes. Strikingly, possible repair mechanisms from newly generated oligodendrocytes are evident in APPPS1 mice, while a similar reaction of oligodendrocyte progenitors seems to be strongly limited in final stages of human AD pathology.

Introduction

Alzheimer's disease (AD) is a neurodegenerative disease in which patients develop progressive cognitive impairment. Pathologically, AD is characterized by the deposition of extracellular plaques that predominantly consist of aggregated Aβ peptides, by the formation of intraneuronal neurofibrillary tangles as well as synapse and focal neuronal loss (Duyckaerts et al. 2009).

In addition to the neuronal phenotype, AD patients show myelin loss both in the cortical gray (GM) and white matter (WM; Roher et al. 2002, Svennerholm and Gottfries 1994, Vlkolinsky et al. 2001) as well as a reduction in size of the corpus callosum (Hampel et al. 1998) and oligodendrocyte cell death (Lassmann et al. 1995). In general, AD patients display an increase in myelin breakdown (Bartzokis et al. 2003). The above observations are highly relevant, since myelin aberrations and loss can lead to a failure of action potential conductance, with the concomitant consequences for the progression of AD-induced impairment.

A potential source for myelin repair could be the cells of the oligodendrocyte lineage and specifically the oligodendrocyte progenitor cells (OPCs). Interestingly, OPCs expressing the proteoglycan NG2 and the transcription factor Olig2 have been detected in the adult, healthy human brain (Geha et al. 2010). Furthermore, these cells represent the only proliferating cell type in the adult brain parenchyma not only in humans but also in mice (Dimou et al. 2008; Geha et al. 2010; Simon et al. 2011). Another important feature of OPCs is their capability to generate myelinating oligodendrocytes in the healthy rodent brain (Dimou et al. 2008; Kang et al. 2010; Rivers et al. 2008; Zhu et al. 2011). Notably, these cells also have a repair potential as they can differentiate into mature oligodendrocytes and consequently remyelinate axons in demyelinating mouse models (Fancy et al. 2011; Fancy et al. 2004; Franklin and Ffrench-Constant 2008; Islam et al. 2009; Zawadzka et al. 2010). Interestingly, although studies using transgenic mice displaying different features of the human AD pathology have shown similar myelin defects to those described in AD patients (Desai et al. 2009; Games et al. 1995; Gonzalez-Lima et al. 2001; Oddo et al. 2003), the reparative

potential of OPCs in these models has yet to be investigated. Moreover, myelin integrity has been mainly analyzed in an AD mouse model that displays AD-associated mutations not only in neurons but also in the oligodendrocyte lineage (3xTg, Desai et al. 2009). As in these mice the PS1-mutation is also expressed in glial cells this could lead to a direct effect of the mutations on OPCs/oligodendrocytes survival, differentiation and myelination due to a loss or gain of function of the mutated protein in these cells (Desai et al. 2011; Horiuchi et al. 2010; Pak et al. 2003a; Pak et al. 2003b; Xu et al. 2001). Therefore, we aimed to analyze the (direct or indirect) effects of extracellular plaque deposition independent of mutations present within the oligodendrocyte lineage by using the APPPS1 mouse model. These mice overexpress mutated forms of the human amyloid precursor protein (APP) and presenilin 1 (PS1) exclusively in postnatal neurons (Radde et al. 2006). This model therefore allows the examination of myelin and cells of the oligodendrocyte lineage in an amyloidosis environment. As this model rather mimics a sporadic etiology of AD we further analyzed cells of the oligodendrocyte lineage in sporadic cases of AD patients.

Materials and Methods

Animals

APPPS1 mice were raised on a heterozygous background by crossing them to C57Bl/6 mice (Radde et al. 2006). All animal procedures were performed in accordance with the policies of the use of Animals and Humans in Neuroscience Research, revised and approved by the Society of Neuroscience and the state of Bavaria under license number: 55.2-1-54-2531-144-07.

To label proliferating cells 1 mg/ml 5-bromo-2-deoxyuridine (BrdU; Sigma Aldrich) supplied with 1% sucrose was administered to mice via the drinking water for 14 consecutive days.

Electron Microscopy

Animals were deeply anaesthetized and transcardially perfused using freshly prepared fixative (2 % paraformaldehyde (PFA); 2.5 % glutaraldehyde in 0,1 M cacodylate buffer (Diemethylarsinic acid sodium salt trihydrate and CaCl dehydrate)). Directly after perfusion brains were dissected, postfixed for 12 hours and kept in cacodylate buffer at 4 °C until further processing. Small pieces were dissected from the cortical gray and white matter and subsequently incubated for 3 hours in 2 % osmium tetroxide at room temperature. The tissue was then dehydrated in graded ethanol, immersed in propylene oxide, and embedded in araldite (araldite epoxy embedding kit; Fluka) following the manufacturer's protocol. Polymerization was performed at 60°C for 2 days. Semi-thin cross-sections of 0.5 µm in thickness were cut for light microscopy inspection, whereas ultrathin sections of 65-85 nm were cut and contrasted with uranylacetate and plumb for electron microscopy analysis with the transmission electron microscope (Phillips CM10). Pictures were taken in the gray and white matter.

Western Blot

Western blot analysis was performed as previously described (Robel et al. 2009). Membranes were probed with the anti-2`3`-cyclic nucleotide 3`-phosphodiesterase (CNPase) antibody (mouse, 1:1000, Sigma) and anti-neurofilament 70 (NF70; mouse 1:1000, Millipore). For protein loading control, membranes were reprobed with anti-Glyceraldehyde 3-phosphate dehydrogenase antibody (GAPDH; mouse, 1:7500, Abcam). For quantification the Odyssey V3.0 software was employed to calculate the pixels of each band by subtraction of the background signal. A minimum of 4 blots/ animal were performed with at least 3 animals per condition and age. In every blot the mean ratio of all controls was set at 100%. The percentage of the ratio was then calculated for the APPPS1 samples on the same blot. Quantification was performed using the one sample t–test.

Histological Analysis of Mouse Tissue Samples

Mice were anaesthetized and transcardially perfused with 4% PFA. Brains were collected and cryoprotected in 30% sucrose. Thirty-micrometer-thick brain sections were cut and stained according to standard protocols as previously described (Dimou et al. 2008; Simon et al. 2011) with the primary antibodies listed in Table 1.

For Olig2 and BrdU immunostaining, pre-treatment of the sections in 0.01 M sodium citrate (pH 6) at 95 °C for 20 minutes was performed. The method for the Gallyas silver impregnation has been described previously (Gallyas, 1971; Gallyas, 1979). The sections were coverslipped with DPX (Fluka) mounting medium.

Human Brain tissue samples

Human brain tissue was obtained from the Neurological Foundation of the New Zealand Human Brain Bank (Department of Anatomy with Radiology and Centre for Brain Research, University of Auckland). Protocols used in this study were approved by the Human Participants Ethics Committee. Brain tissue (Table 2) was obtained with full consent of the families from 8 neurologically normal cases with neither history nor evidence of neuropathology as well as from 8 AD cases. The average age was 73 years with a range of 35-85 years. The cases had a post-mortem interval between 2 and 36 hours after death (mean post-mortem interval 14.75 hrs) and included 8 females and 8 males. For details please see Table 2.

Histological Analysis of Human Tissue Samples

The human brain sections cut at 50 μm were processed for immunohistochemical staining as previously described (Waldvogel et al. 2006). In short, adjacent free-floating sections were processed for antigen retrieval incubated with anti-human OLIG2 antibody (rabbit, 1:500, Santa Cruz) was followed by a species-specific biotinylated secondary antibody (sheep anti-rabbit, 1:500, Chemicon, USA). After washing, sections were incubated for 4 hours at room temperature in ABC solution (1:250, Vectastain). Sections were then incubated in 0.05 % 3,3-diaminobenzidine tetrahydrochloride (DAB; Sigma) and 0.01 % H_2O_2 in 0.1 M phosphate

buffer, pH 7.4, for 15-20 minutes to produce a brown reaction product. A nickel-intensified procedure was used in which 0.4 % nickel ammonium sulphate was added to the DAB solution to produce a blue-black reaction product (Adams, 1981). The sections were washed in phosphate buffered saline (PBS), mounted on gelatine chrome-alum coated slides, rinsed in distilled water, dehydrated, and coverslipped with DPX (BDH, Poole, UK). Control sections were routinely processed to determine non-specific staining using the same immunohistochemical procedures described above except that the primary antibody was omitted.

Quantifications

Mouse samples

Quantification of rodent myelin integrity at the ultrastructural level was performed at a magnification of 11440x in the Phillips CM10 electron microscope. At least 10 pictures per animal and 3-4 mice per genotype and age were analyzed by two independent persons and the mean of aberrations per axon were calculated for every picture.

Immunostainings of mouse tissue were analyzed at the Zeiss LSM700 confocal microscope with a z-stack between 6-7 µm. At least three sections from areas +1, 0 and -2 from the bregma (anterior-posterior) and two adjacent fields of view including all gray matter layers were quantified. The area of interest was measured and cells were quantified using the Image J software. Statistical analysis was performed with the Graph Pad Prism program. Quantification of immunolabeled cells in mice was performed in a minimum of 3 sections per animal, from more than 3 animals and tested for normal distribution using then, depending on the data distribution, either the unpaired Student's t-test or the Mann-Whitney test (* $p< 0.05$; ** $p< 0.01$; *** $p < 0.001$). Significant changes are indicated in the diagram bars and data are represented as ±SEM.

Human samples

Single human tissue sections were examined by light microscopy using a Zeiss Axioscope. Digital images were captured and contrast optimized using ImageJ software (NIH) and quantitative observations were recorded. Statistical analysis was carried out using Excel and Minitab software. Three independent rounds of staining were performed, each time using one brain section from 3-5 healthy control brains and from 3-5 AD brains. Per brain section, using the 4x magnification, a minimum of 3 digital pictures was captured from the white and from the gray matter. The digital pictures were coded and the quantification (counting of OLIG2+ nuclei) was carried out using the cell counter of the ImageJ software (NIH). Quantification of immunolabeled cells was determined in pictures from more than 3 cases per group and tested with the Mann-Whitney test (* $p< 0.05$; ** $p< 0.01$; *** $p < 0.001$).

Results

Focal loss of myelin in plaque core areas in APPPS1 mice

In this study we took advantage of the APPPS1 mouse line that overexpresses mutated forms of the human APP and PS1 under the control of the neuron-specific Thy1 promoter element. These mice reflect certain clinical aspects of Alzheimers Disease (AD), since they exhibit progressive amyloid plaque deposition in all brain regions starting in the cortical gray matter at 6 weeks of age. Plaque deposition is accompanied by robust gliosis and neuritic hyperphosphorylated tau, while tangle formation and obvious cortical neuronal degeneration are not reported in these mice (Radde et al., 2006; Rupp et al., 2010).To analyze changes in myelin distribution we stained brain sections of transgenic (APPPS1) and wild type littermates for the myelin associated glycoprotein (MAG) at 6 and 11 months of age (Fig. 1G), when plaque deposition has developed already for some months (Suppl. Fig. 1). Additionally, we performed a Gallyas impregnation to label myelin independently of any specific antigen expression. Both techniques revealed focal demyelination in the plaque core areas of the cerebral gray matter (GM; Fig. 1A, B, D, E) and to a lesser extent in the white

matter (WM; Fig. 1C, F) which is in accordance with observations in human patient samples (Mitew et al. 2010).

To quantify the myelin amount in relation to the axons at different ages, we performed Western blot analysis with antibodies raised against the oligodendrocytic protein 2',3'-cyclic nucleotide 3'-phosphodiesterase (CNP) and the axonal neurofilament 70 (NF70). At 6 months of age, when plaque deposition is obvious, significantly less CNP was present in relation to the axonal NF70 in APPPS1 compared to control mice, while at 9 months of age this ratio was similar to wildtype animals (Fig. 1 H, I).

Increase in myelin aberrations in 6 month old APPPS1 mice

In order to examine myelin integrity in the APPPS1 mice we performed ultrastructural analysis by electron microscopy in the GM and WM of the cerebral cortex. Analysis of 6 months old animals revealed a higher number of myelin aberrations in both cortical GM (Fig. 2B-F; Fig. 2A wild type control) and WM (Fig. 2H-L; Fig. 2G wildtype control). Myelin aberrations were classified according to criteria described in Peters et al. (2000) and Thurnherr et al. (2006), as e.g. an axon surrounded by two myelin sheaths (Fig. 2D, J), excess cytoplasm in the inner loop (Fig. 2K), degenerated sheaths (Fig. 2E), balooned myelin (Fig. 2F, L), abnormal myelin outfoldings (Fig. 2C, I), which we defined as areas of the internode where the myelin sheath protruded away from the axon surface, or other myelin abnormalities (Fig. 2B, H). Given the lower number of myelinating axons in the GM, we focused our quantitative analysis of myelin aberrations in the WM and determined the percentage of defects per axonal number in the corpus callosum. This revealed a significantly higher proportion of axons with aberrant myelin in the APPPS1 mice compared to control littermates (Fig. 2M), while the myelin compaction was normal (data not shown). In contrast, no significant difference in the proportion of axons with aberrant myelin was observed in 9 months old mice (Fig. 2M), which is in line with the normalized value of CNPase/NF70 ratio. Notably, control animals showed a progressive increase in myelin aberrations between 6 and 9 months as reported in aging rhesus monkeys (Bowley et al.

2010) while APPPS1 mice did not indicate any further age-dependent elevation in myelin defects within the same time period.

To investigate whether the observed aberrations in 6 month old animals arise during development or are associated with the plaques appearance, we analyzed myelin formation and integrity in 3 month old animals, an age when plaque deposition starts and myelination is almost completed. Gallyas silver impregnation as well as measurement of the corpus callosum (CC)-thickness did not reveal any obvious differences between control and APPPS1 mice (data not shown). Likewise, ultrastructural analysis of myelin integrity in the WM showed no differences in number of myelin aberrations between 3 month old APPPS1 and age matched control mice (Fig. 2M).

We can therefore conclude that the myelin aberrations observed in 6 month old animals are not due to dysmyelination from early postnatal development but rather developed at later stages correlating with the plaque load.

Number of cells expressing the transcription factor Olig2 is increased in the gray matter of 6 months old APPPS1 mice

Given the increased incidence of myelin aberrations in APPPS1 mice at 6 months of age, we asked to which extent cells of the oligodendrocyte lineage react to plaque load. As all OPCs are Olig2-immunoreactive (Karram et al. 2008; Zhou et al. 2000) and only little overlap was found with S100β/GFAP+ astrocytes (Fig. 3C), we quantified Olig2+ cells in the cortical GM of 3, 6 and 11 months old animals. While no differences between genotypes were detected in the cerebral cortex of 3 month old mice, a time point when the first plaques appear (Fig. 3B; Suppl. Fig. 1), the number of Olig2+ cells was significantly increased in 6 and 9 month old APPPS1 mice (Fig. 3A, B) . From these data we can conclude that amyloid plaque deposition precedes the transient increase of Olig2+ cell number in 6 months old animals, an age that correlates with the elevation in myelin aberrations.

Since Olig2 is expressed in a variety of cell types in different lesion paradigms we aimed to assess which cells may be responsible for the increased number of Olig2+ cells in the GM of

6 months old APPPS1 mice. Therefore, we co-stained Olig2 with NG2 to detect OPCs, GSTπ for mature oligodendrocytes (Tansey and Cammer, 1991) and S100β/GFAP for astrocytes. Interestingly, while the number of mature, GSTπ+ oligodendrocytes remained stable at 6 months of age, we observed a significant increase of NG2+ OPCs in the APPPS1 mice (Fig. 3C). Notably, also the number of Olig2+ astrocytes increased in the transgenic animals but still represented a minor population of all Olig2+ cells (8.9 ± 0.9 double-positive cells/mm^2 in control and 19.3 ± 2.6 in APPPS1 mice).

Increase in proliferation of oligodendrocyte progenitors and generation of mature oligodendrocytes in the cortical gray matter

To test whether the increased number of Olig2+/NG2+ cells is due to changes in proliferation, the animals received BrdU -a thymidine analog that incorporates into the DNA during cell division- in the drinking water for 2 weeks and were then directly sacrificed. With this protocol we labeled slow and fast proliferating cells as well as cells that have divided and become post-mitotic within this time period. At the age of 3 months the same number of Olig2+/BrdU+ cells was observed in the cerebral cortex of wild type and APPPS1 mice (Fig. 3D). In contrast and consistent with our previous observations, we found an increase in the number of Olig2+/BrdU+ cells in APPPS1 mice at 6 months that remained obvious at 11 months of age (Fig. 3D). Thus, the increase in the number of Olig2+ cells in APPPS1 mice is likely to be the result of enhanced proliferation of these cells. Interestingly, the number of proliferating Olig2+ cells in control animals significantly decreased with age (between 3 and 11 months) as it has also been observed for proliferating cells in the neurogenic niches in aging mouse brain (Lazarov et al. 2010).

To trace OPCs and their progeny directly, we first monitored proliferation of OPCs by 2 weeks BrdU application and then analyzed their progeny 4 weeks later. The number of proliferating NG2+ cells was increased about 2-fold in the cerebral cortex GM of 6 months old APPPS1 mice compared to controls (Fig. 4A, B). The increased proliferation of NG2+ OPCs could be a reaction to the focal loss of myelin and increasing plaque load in the GM

and an attempt to repair and replace oligodendrocytes. Indeed, when the progeny of these proliferating cells was analyzed 4 weeks later, we detected a 2.5-fold increase in the generation of mature GSTπ+ oligodendrocytes in the APPPS1 mice (Fig. 4C, D). This enhanced maturation of OPCs hints at an increased generation of oligodendrocytes possibly contributing to myelin repair as a response to the focal demyelination and the transient decrease in myelin amount.

Increased proliferation and differentiation of OPCs in the white matter of APPPS1 mice at 6 months of age

As myelin aberrations were also identified in the WM of APPPS1 mice, we analyzed the proliferation properties of OPCs and the generation of mature oligodendrocytes in this area. Consistent with the above described increase in NG2+ cell proliferation in the GM, these cells also increased their proliferation in the WM by 1.5-fold in 6 month old APPPS1 mice (Fig. 5A). Likewise, also their differentiated progeny (BrdU+/GSTπ+ cells) examined 1 month later was increased by 2-fold in the APPPS1 mice (Fig. 5B-D). Notably, the number of NG2+ progenitors as well as newly generated oligodendrocytes in the WM was much higher compared to the GM in control and APPPS1 mice consistent with the higher density of cells of the oligodendrocyte lineage in the WM.

In summary, the elevated number of myelin aberrations correlates with an increase in proliferation of OPCs followed by a subsequent increase in their differentiation into mature oligodendrocytes.

Decrease in number of OLIG2+ cells in human Alzheimer's disease

The previous results indicated a specific response of cortical oligodendrocyte progenitors and a subsequent increase in generation of mature oligodendrocytes in a chronic amyloid plaque deposition mouse model. However, cells belonging to the oligodendrocyte lineage have been poorly investigated in human AD. In order to examine whether a similar response of Olig2+ cells (both OPCs and mature oligodendrocytes) observed in mice is also present in

human AD pathology, we assessed the number of OLIG2-expressing cells in the gray and white matter of human post-mortem cerebral cortex tissue from neurologically healthy and AD cases (8 subjects per group; for detailed information to the human cases see Table 2). We also focused on the same cortical region as in the mouse model, the pre- and postcentral gyri of the sensory motor cortex (Fig. 6A-D). Surprisingly, we observed a large decrease in the number of OLIG2+ cells in both GM (Fig. 6A, C) and WM (Fig. 6B, D) of AD sensory motor cortex (SM).

Since the SM is not predominantly affected in human AD patients, we also quantified the number of OLIG2+ cells in the GM and WM of the Superior Temporal Gyrus (STG; Fig. 6E, F) and Mid Frontal Gyrus (MFG; Fig. 6G, H), two other cortical areas affected in early AD pathology. In both areas we detected a decrease in the number of OLIG2+ cells as observed in the sensory motor cortex, except in the WM of the MFG where the number of OLIG2+ cells was even increased (Fig. 6H). To further confirm that the observed overall reduction of OLIG2-expressing cells in AD cerebral cortex is not due to neuronal and subsequential loss of oligodendrocytes, we quantified the percentage of OLIG2+ cells per total number of cells (DAPI+ nuclei) in the GM and WM of human SM, STG and MFG cortex (Suppl. Fig. 2A-F). As observed for the absolute number, the percentage of OLIG2+ cells was significantly reduced in the SM, STG and MFG cortex tissue, suggesting a specific reduction of OLIG2+ cells in AD patients. The only exception was again the white matter of the MFG, where the percentage of OLIG2+/DAPI+ cells was similar between normal and AD cases (Suppl. Fig. 2F).

Discussion

Transient Alterations in Myelin in APPPS1 Mice Here, we demonstrated that in the APPPS1 mice, a mouse model of AD with plaque depositions myelin alterations can be induced. Since in contrast to other AD mouse models the mutations in APP and PS1 are exclusively expressed in neurons, we can exclude direct effects of the mutations in cells of

the oligodendrocyte lineage. Indeed, PS1 mutations in oligodendrocytes can increase their vulnerability towards different stressors such as e.g. glutamate and amyloid beta peptide (Aβ) (Desai et al. 2011; Pak et al. 2003a; Pak et al. 2003b). This may explain why in the 3xTg mice (for details about the mouse line see Table 3), which ubiquitously express the PS1 mutation including cells of the oligodendrocyte lineage, myelin aberrations are observed even before plaque deposition becomes visible (Desai et al. 2009).

As APPPS1 mice also express mutated APP protein exclusively in neurons, transgenic expression of this mutation might affect myelination by axon-mediated signaling to oligodendrocytes. For example PDAPP mice, that express an APP mutation preferentially in neurons already embryonically, show hypomyelination by postnatal day 40 which is still present until at least 21 months of age (Redwine et al. 2003). The early appearance of this phenotype is thus most likely caused by the prenatal expression of the APP mutation driven by the PDGFβ-promoter in this mouse line (Games et al. 1995; see Table 3). Conversely, the APP mutation in our mouse model is only expressed postnatally (around P14). Accordingly, myelination was normal until 3 months of age, excluding any developmental defects and alterations in myelination due to impaired axonal-oligodendrocyte communication.

Furthermore in our mice, the degree of myelin alterations correlated to the extent of plaque deposition. In 4-5 month old APPPS1 mice 35 new plaques (per mm^3) develop every week, while the number of newly formed plaques decreases at later ages (Hefendehl et al. 2011). Hence, the peak of myelin aberrations detected in our study at 6 months of age corresponds well with the peak of plaque formation. However, whether there is a direct or indirect effect of the plaques on myelin maintenance is still unknown. Anyway, it seems that amyloid deposition does not affect the generation of new oligodendrocytes. This could be explained either by different effects of amyloid on myelinating oligodendrocytes and OPCs or a decreased vulnerability of the newly generated oligodendrocytes. Additionally, the fact that not all myelin sheaths are affected could also point to a heterogeneity of oligodendrocytes that react differently to the amyloid plaques.

In conclusion, the myelin aberrations reported in our study are not the result of direct effects of gene mutations in oligodendrocytes but rather the direct or indirect effect of the extracellular plaque deposition or the mutated neurons. This is of great importance as mutations of these genes in all cells, including cells of the oligodendrocyte lineage, have been solely reported in familial cases of AD that only constitute 5-10% of all AD cases (Castellani et al. 2010). Studying specifically myelin integrity in "healthy" oligodendrocytes will improve our understanding on the influence of this pathology in the sporadic AD patients that constitute the vast majority of all AD cases.

Indications for Myelin Repair upon Chronic Plaque Deposition

The increased generation of mature oligodendrocytes in 6-8 month old APPPS1 mice may lead to the equalization of myelin aberrations between APPPS1 and control mice at 9 months of age.

It has been shown that large diameter remyelinated fibers, in contrast to small diameter axons, can be recognized by thinner and less compacted myelin sheaths (Blakemore, 1974; Prineas et al. 1993). Since in our study we analyzed callosal axons that belong to the small diameter fibers and thus do not directly give evidence for remyelination (Franklin and Ffrench-Constant, 2008), a morphological identification of newly generated myelin sheaths in ultrastructural pictures was not possible

However, BrdU labeling revealed a clear increase in newly generated mature oligodendrocytes in the GM and WM strongly suggesting that these cells may contribute to alleviate myelin aberrations as observed at 9 months of age. Moreover, increased OPC proliferation followed by increased differentiation precedes remyelination of axons in demyelination models (Fancy et al. 2004; Talbott et al. 2005).

The signals mediating the increase in OPCs proliferation are still unknown. Focal demyelination or the aberrantly myelinated axons themselves may trigger enhanced proliferation in the APPPS1 mice. Also in other lesion models, like the stab wound injury, where both axons and myelin are affected, OPCs similarly react with enhanced proliferation

(Simon et al. 2011). However, the response of NG2+ cells in the APPPS1 mice may not only be triggered by demyelination, but also by other stimuli. For example, microglia that become reactive upon acute lesion as well as chronic plaque deposition (Bolmont et al. 2008) can trigger OPC reactivity (Glezer et al. 2006). Furthermore, Aβ itself may influence myelin formation in APPPS1 mice as its application to rat oligodendrocyte cultures reduces the survival of mature oligodendrocytes and inhibits myelin sheath formation (Horiuchi et al. 2010). In addition, also OPC survival is affected by Aβ under certain conditions (Desai et al. 2010). Here, we detected an increase in proliferation and differentiation of OPCs at a time point when Aβ is already present, indicating that in our mouse model Aβ is either stimulating OPC survival or affecting OPCs proliferation in an indirect manner.

Decrease in the number of OLIG2+ cells in human Alzheimer's disease

Our results revealed important differences in the reaction of Olig2+ cells between the APPPS1 mouse model and human post-mortem AD cortex. While the number of Olig2-expressing cells was increased in 6 months old APPPS1 mice, it was decreased in human post-mortem AD tissue. Different explanations for this observation could be possible. The number of Olig2+ cells was quantified at different ages and disease stages in human and mice. While we studied relatively aged human brains, mice were analyzed at adult stages but not in the last period of their lifespan. Thus, it is possible that the number of Olig2+ cells may also decline in aged AD mouse models and then further resemble the human pathology as already described for the Tg2579 mice (see Table 3 for details), where the number of Olig2+ cells decreases at the age of 15-20 months (Uchida et al. 2007). We additionally observed a decrease in proliferation of OPCs with age (as shown in the 11 months old control mice) that could explain an age-related reduction in cells of the oligodendrocyte lineage (OLIG2+) also in the human brain. The decrease in the proliferation capacity of cortical precursors further correlates with a significant reduction in proliferation in the adult neurogenic niches (Lazarov et al. 2010).

As the amount of myelin changes with age, the time point of analysis is of particular relevance. In humans, myelin content in the frontal lobe white matter reaches its peak in middle age (approximately 45 years of age; Bartzokis et al. 2001) while age-related myelin breakdown occurs at later stages. Likewise, the efficiency of remyelination in a rat model of demyelination decreases with age (Sim et al. 2002) suggesting an age-related reduction in myelin repair capacity that may also occur in AD patients.

Also the disease stages analyzed are different between mice and human, therefore it is possible that the number of Olig2+ cells changes with progression of the disease. Indeed, in our human samples, we observed a negative correlation between the severity of the disease and the number of OLIG2+ cells with the most severe AD cases displaying the lowest number of OLIG2+ cells (data not shown). Moreover, there are differences between human individuals (such as degree of atrophy and the presence of plaques and tangles) and AD mouse models that are inbred and uniformly treated to minimize individual differences.

In conclusion, OPCs that have the ability to repair myelin defects are a promising therapeutic target to improve impairments not only in AD patients but also in other neurodegenerative diseases as myelin breakdown and loss of myelin can result in similar behavioral and cognitive symptoms despite entirely different etiologies (Bartzokis, 2004; Bartzokis, 2011). Therefore, therapeutic interventions at early stages of these diseases that either prevent demyelination or enhance repair/regeneration efficiency would be of great importance. The APPPS1 mice are a suitable model to study and identify factors that stimulate proliferation and differentiation of OPCs as a result of plaque formation. As OPCs are also present in the human brain, factors mediating their response in mice could also be applied in humans to ameliorate a patients' neurological condition.

Acknowledgements

We thank Gabriele Jäger, Simone Bauer, Johanna Zaisserer and Sabine Tost for excellent technical assistance and Jennifer Price for help with statistical analysis of human cortical tissue. We also like to thank the Graduate School of Systemic Neurosciences for support and funding. This work was mainly supported by the Breuer Stiftung and the SFB 596 of the Deutsche Forschungsgemeinschaft. Additional support was obtained by the SFB 870, the Helmholtz Association of mental aging (HELMA) and the Friedrich Bauer Stiftung as well as the Royal Society (KB and MIR) and the National Institute of Social Care and Health Research (NISCHR – MIR). The brain collection and processing was supported by the Neurological Foundation of New Zealand and the Health Research Council of New Zealand.

References

Adams JC. 1981. Heavy metal intensification of DAB-based HRP reaction product. J Histochem Cytochem 29(6): 775.

Bartzokis G. 2004. Age-related myelin breakdown: a developmental model of cognitive decline and Alzheimer's disease. Neurobiology of aging 25(1): 5-18; author reply 49-62.

Bartzokis G. 2011. Alzheimer's disease as homeostatic responses to age-related myelin breakdown. Neurobiology of aging 32(8): 1341-71.

Bartzokis G, Beckson M, Lu PH, Nuechterlein KH, Edwards N, Mintz J. 2001. Age-related changes in frontal and temporal lobe volumes in men: a magnetic resonance imaging study. Arch Gen Psychiatry 58(5): 461-5.

Bartzokis G, Cummings JL, Sultzer D, Henderson VW, Nuechterlein KH, Mintz J. 2003. White matter structural integrity in healthy aging adults and patients with Alzheimer disease: a magnetic resonance imaging study. Arch Neurol 60(3): 393-8.

Blakemore WF. 1974. Pattern of remyelination in the CNS. Nature 249(457): 577-8.

Bolmont T, Haiss F, Eicke D, Radde R, Mathis CA, Klunk WE, Kohsaka S, Jucker M, Calhoun ME. 2008. Dynamics of the Microglial/Amyloid Interaction Indicate a Role in Plaque Maintenance. J Neurosci. 2008; 28(16): 4283-92.

Bowley MP, Cabral H, Rosene DL, Peters A. 2010. Age changes in myelinated nerve fibers of the cingulate bundle and corpus callosum in the rhesus monkey. J Comp Neurol 518(15): 3046-64.

Castellani RJ, Rolston RK, Smith MA. 2010. Alzheimer Disease. Dm-Dis Mon 56(9): 484-546.

Desai MK, Guercio BJ, Narrow WC, Bowers WJ. 2011. An Alzheimer's disease-relevant presenilin-1 mutation augments amyloid-beta-induced oligodendrocyte dysfunction. Glia 59(4): 627-40.

Desai MK, Mastrangelo MA, Ryan DA, Sudol KL, Narrow WC, Bowers WJ. 2010. Early Oligodendrocyte/Myelin Pathology in Alzheimer's Disease Mice Constitutes a Novel Therapeutic Target. Am J Pathol 177(3):1422-35.

Desai MK, Sudol KL, Janelsins MC, Mastrangelo MA, Frazer ME, Bowers WJ. 2009. Triple-transgenic Alzheimer's disease mice exhibit region-specific abnormalities in brain myelination patterns prior to appearance of amyloid and tau pathology. Glia 57(1): 54-65.

Dimou L, Simon C, Kirchhoff F, Takebayashi H, Gotz M. 2008 Progeny of Olig2-expressing progenitors in the gray and white matter of the adult mouse cerebral cortex. J Neurosci 28(41): 10434-42.

Dodart JC, Mathis C, Saura J, Bales KR, Paul SM, Ungerer A. 2000. Neuroanatomical abnormalities in behaviorally characterized APP(V717F) transgenic mice. Neurobiology of disease. 2000; 7(2): 71-85.

Duyckaerts C, Delatour B, Potier MC. Classification and basic pathology of Alzheimer disease. Acta Neuropathol 118(1): 5-36.

Fancy SP, Chan JR, Baranzini SE, Franklin RJ, Rowitch DH. 2011 Myelin regeneration: a recapitulation of development? Annual review of neuroscience 34: 21-43.

Fancy SP, Zhao C, Franklin RJ. 2004. Increased expression of Nkx2.2 and Olig2 identifies reactive oligodendrocyte progenitor cells responding to demyelination in the adult CNS. Mol Cell Neurosci 27(3): 247-54.

Franklin RJ, Ffrench-Constant C. 2008. Remyelination in the CNS: from biology to therapy. Nat Rev Neurosci 9(11): 839-55.

Gallyas F. 1971. A principle for silver staining of tissue elements by physical development. Acta Morphol Acad Sci Hung 19(1): 57-71.

Gallyas F. 1979. Silver staining of myelin by means of physical development. Neurol Res 1(2): 203-9.

Games D, Adams D, Alessandrini R, Barbour R, Berthelette P, Blackwell C, et al. 1995. Alzheimer-type neuropathology in transgenic mice overexpressing V717F beta-amyloid precursor protein. Nature 373(6514): 523-7.

Geha S, Pallud J, Junier MP, Devaux B, Leonard N, Chassoux F, Chneiweiss H, Daumas-Duport C, Varlet P. 2010. NG2+/Olig2+ cells are the major cycle-related cell population of the adult human normal brain. Brain Pathol 20(2): 399-411.

Glezer I, Lapointe A, Rivest S. 2006. Innate immunity triggers oligodendrocyte progenitor reactivity and confines damages to brain injuries. Faseb J 20(6): 750-2.

Gonzalez-Lima F, Berndt JD, Valla JE, Games D, Reiman EM. 2001. Reduced corpus callosum, fornix and hippocampus in PDAPP transgenic mouse model of Alzheimer's disease. Neuroreport 12(11): 2375-9.

Hampel H, Teipel SJ, Alexander GE, Horwitz B, Teichberg D, Schapiro MB, Rapoport SI. 1998. Corpus callosum atrophy is a possible indicator of region- and cell type-specific neuronal degeneration in Alzheimer disease: a magnetic resonance imaging analysis. Arch Neurol 55(2): 193-8.

Hefendehl JK, Wegenast-Braun BM, Liebig C, Eicke D, Milford D, Calhoun ME, Kohsaka S, Eichner M, Jucker M. 2011. Long-term in vivo imaging of beta-amyloid plaque appearance and growth in a mouse model of cerebral beta-amyloidosis. J Neurosci 31(2): 624-9.

Horiuchi M, Maezawa I, Itoh A, Wakayama K, Jin LW, Itoh T, Decarli C. 2012. Amyloid beta1-42 oligomer inhibits myelin sheet formation in vitro. Neurobiology of aging 33(3):499-509

Hsiao K, Chapman P, Nilsen S, Eckman C, Harigaya Y, Younkin S, Yang F, Cole G. 1996. Correlative memory deficits, Abeta elevation, and amyloid plaques in transgenic mice. Science 274(5284): 99-102.

Irizarry MC, McNamara M, Fedorchak K, Hsiao K, Hyman BT. 1997. APPSw transgenic mice develop age-related A beta deposits and neuropil abnormalities, but no neuronal loss in CA1. Journal of neuropathology and experimental neurology 56(9): 965-73.

Islam MS, Tatsumi K, Okuda H, Shiosaka S, Wanaka A. 2009. Olig2-expressing progenitor cells preferentially differentiate into oligodendrocytes in cuprizone-induced demyelinated lesions. Neurochem Int 54(3-4): 192-8.

Kang SH, Fukaya M, Yang JK, Rothstein JD, Bergles DE. 2010. NG2+ CNS glial progenitors remain committed to the oligodendrocyte lineage in postnatal life and following neurodegeneration. Neuron 68(4): 668-81.

Karram K, Goebbels S, Schwab M, Jennissen K, Seifert G, Steinhauser C, Nave KA, Trotter J. 2008. NG2-expressing cells in the nervous system revealed by the NG2-EYFP-knockin mouse. Genesis 46(12): 743-57.

Larson J, Lynch G, Games D, Seubert P. 1999. Alterations in synaptic transmission and long-term potentiation in hippocampal slices from young and aged PDAPP mice. Brain research 840(1-2): 23-35.

Lassmann H, Bancher C, Breitschopf H, Wegiel J, Bobinski M, Jellinger K, Wisniewski HM. 1995. Cell death in Alzheimer's disease evaluated by DNA fragmentation in situ. Acta Neuropathol 89(1): 35-41.

Lazarov O, Mattson MP, Peterson DA, Pimplikar SW, van Praag H. 2010. When neurogenesis encounters aging and disease. Trends in Neurosciences 33(12): 569-79.

Manson J, West JD, Thomson V, McBride P, Kaufman MH, Hope J. 1992. The prion protein gene: a role in mouse embryogenesis? Development 115(1): 117-22.

Mitew S, Kirkcaldie MT, Halliday GM, Shepherd CE, Vickers JC, Dickson TC. 2010. Focal demyelination in Alzheimer's disease and transgenic mouse models. Acta Neuropathol 119(5): 567-77.

Oddo S, Caccamo A, Shepherd JD, Murphy MP, Golde TE, Kayed R, Metherate R, Mattson MP, Akbari Y, LaFerla FM. 2003. Triple-transgenic model of Alzheimer's disease with plaques and tangles: intracellular Abeta and synaptic dysfunction. Neuron 39(3): 409-21.

Pak K, Chan SL, Mattson MP. 2003a. Presenilin-1 mutation sensitizes oligodendrocytes to glutamate and amyloid toxicities, and exacerbates white matter damage and memory impairment in mice. Neuromolecular Medicine 3(1): 53-64.

Pak KJ, Chan SL, Mattson MP. 2003b. Homocysteine and folate deficiency sensitize oligodendrocytes to the cell death-promoting effects of a presenilin-1 mutation and amyloid beta-peptide. Neuromolecular Medicine 3(2): 119-27.

Peters A, Moss MB, Sethares C. 2000. Effects of aging on myelinated nerve fibers in monkey primary visual cortex. Journal of Comparative Neurology 419(3): 364-76.

Prineas JW, Barnard RO, Kwon EE, Sharer LR, Cho ES. 1993. Multiple sclerosis: remyelination of nascent lesions. Ann Neurol 33(2): 137-51.

Radde R, Bolmont T, Kaeser SA, Coomaraswamy J, Lindau D, Stoltze L, Calhoun ME, Jäggi F, Wolburg H, Gengler S, Haass C, Ghetti B, Czech C, Hölscher C, Mathews PM, Jucker M. 2006 . Abeta42-driven cerebral amyloidosis in transgenic mice reveals early and robust pathology. EMBO Rep 7(9): 940-6.

Redwine JM, Kosofsky B, Jacobs RE, Games D, Reilly JF, Morrison JH, Young WG, Bloom FE. 2003. Dentate gyrus volume is reduced before onset of plaque formation in PDAPP mice: a magnetic resonance microscopy and stereologic analysis. Proc Natl Acad Sci U S A 100(3): 1381-6.

Rivers LE, Young KM, Rizzi M, Jamen F, Psachoulia K, Wade A, Kessaris N, Richardson WD. 2008. PDGFRA/NG2 glia generate myelinating oligodendrocytes and piriform projection neurons in adult mice. Nat Neurosci 11(12): 1392-401.

Robel S, Mori T, Zoubaa S, Schlegel J, Sirko S, Faissner A, Goebbels S, Dimou L, Götz M. 2009. Conditional Deletion of beta 1-Integrin in Astroglia Causes Partial Reactive Gliosis. Glia 57(15): 1630-47.

Roher AE, Weiss N, Kokjohn TA, Kuo YM, Kalback W, Anthony J, Watson D, Luehrs DC, Sue L, Walker D, Emmerling M, Goux W, Beach T. 2002. Increased A beta peptides and reduced cholesterol and myelin proteins characterize white matter degeneration in Alzheimer's disease. Biochemistry 41(37): 11080-90.

Rupp NJ, Wegenast-Braun BM, Radde R, Calhoun ME, Jucker M. 2011. Early onset amyloid lesions lead to severe neuritic abnormalities and local, but not global neuron loss in APPPS1 transgenic mice. Neurobiology of aging 32(12):2324.

Sasahara M, Fries JWU, Raines EW, Gown AM, Westrum LE, Frosch MP, Bonthron DT, Ross R, Collins T. 1991. Pdgf B-Chain in Neurons of the Central-Nervous-System, Posterior Pituitary, and in a Transgenic Model. Cell 64(1): 217-27.

Sim FJ, Zhao C, Penderis J, Franklin RJ. 2002. The age-related decrease in CNS remyelination efficiency is attributable to an impairment of both oligodendrocyte progenitor recruitment and differentiation. J Neurosci 22(7): 2451-9.

Simon C, Götz M, Dimou L. 2011. Progenitors in the adult cerebral cortex: Cell cycle properties and regulation by physiological stimuli and injury. Glia 59(6):869-81.

Svennerholm L, Gottfries CG. 1994. Membrane lipids, selectively diminished in Alzheimer brains, suggest synapse loss as a primary event in early-onset form (type I) and demyelination in late-onset form (type II). J Neurochem 62(3): 1039-47.

Talbott JF, Loy DN, Liu Y, Qiu MS, Bunge MB, Rao MS, Whittemore SR. 2005. Endogenous Nkx2.2+/Olig2+ oligodendrocyte precursor cells fail to remyelinate the demyelinated adult rat spinal cord in the absence of astrocytes. Exp Neurol 192(1): 11-24.

Tansey FA, Cammer W.1991. A pi form of glutathione-S-transferase is a myelin- and oligodendrocyte-associated enzyme in mouse brain. J Neurochem 57(1):95-102.

Thurnherr T, Benninger Y, Wu XW, Chrostek A, Krause SM, Nave KA, Franklin RJ, Brakebusch C, Suter U, Relvas JB. 2006. Cdc42 and Rac1 signaling are both required for and act synergistically in the correct formation of myelin sheaths in the CNS. J Neurosci 26(40): 10110-9.

Uchida Y, Nakano S, Gomi F, Takahashi H. 2007. Differential regulation of basic helix-loop-helix factors Mash1 and Olig2 by beta-amyloid accelerates both differentiation and death of cultured neural stem/progenitor cells. The Journal of biological chemistry 282(27): 19700-9.

Vlkolinsky R, Cairns N, Fountoulakis M, Lubec G. 2001. Decreased brain levels of 2',3'-cyclic nucleotide-3'-phosphodiesterase in Down syndrome and Alzheimer's disease. Neurobiology of aging 22(4): 547-53.

Waldvogel HJ, Curtis MA, Baer K, Rees MI, Faull RL. 2006. Immunohistochemical staining of post-mortem adult human brain sections. Nat Protoc 1(6): 2719-32.

Xu J, Chen S, Ahmed SH, Chen H, Ku G, Goldberg MP, Hsu CY. 2001. Amyloid-beta peptides are cytotoxic to oligodendrocytes. J Neurosci 21(1): RC118.

Zawadzka M, Rivers LE, Fancy SP, Zhao C, Tripathi R, Jamen F, Young K, Goncharevich A, Pohl H, Rizzi M, Rowitch DH, Kessaris N, Suter U, Richardson WD, Franklin RJ. 2010. CNS-resident glial progenitor/stem cells produce Schwann cells as well as oligodendrocytes during repair of CNS demyelination. Cell stem cell 6(6): 578-90.

Zhou Q, Wang S, Anderson DJ. 2000. Identification of a novel family of oligodendrocyte lineage-specific basic helix-loop-helix transcription factors. Neuron 25(2): 331-43.

Zhu X, Hill RA, Dietrich D, Komitova M, Suzuki R, Nishiyama A. 2011. Age-dependent fate and lineage restriction of single NG2 cells. Development 138(4): 745-53.

Table 1: List of Primary Antibodies

Antibody	Host	Dilution	Company
Anti-Aβ/APP	clone 6E10, mouse	1:200	Millipore
anti-Bromodeoxyuridine (BrdU)	rat	1:200	Biozol
anti glial-fibrillary acidic protein (GFAP)	mouse	1:1000	Sigma Aldrich
anti glial-fibrillary acidic protein (GFAP)	rabbit	1:1000	DAKO
anti-Glutathione-S-transferase π (GSTπ)	mouse	1:500	BD Bioscience
anti-NG2	rabbit	1:200	Chemicon
anti-Olig2	rabbit	1:500	Chemicon
anti-S100β	mouse	1:1000	Sigma Aldrich
anti-MAG	mouse	1:100	Chemicon

Table 2: List of human Cases Used in this Study

Case	Age (years)	Sex	Postmortem delay (hours)	Indication - (Cause of death)
H123	78	f	7.5	Control – (Rupt. Aortic aneurysm)
H126	35	f	10	Control – (Suicide/hanging)
H136	75	m	13	Control – (Rupt. Aorta, abdom. Aneurysm)
H137	77	m	12	Control – (Coronary artherosclerosis)
H150	78	m	11	Control – (Rupt. Myocardial infarction)
H191	77	m	20	Control – (Ischaemic heart disease)
H192	65	f	24	Control – (Ischaemic heart disease)
H193	71	m	23	Control – (Ischaemic heart disease)
AZ32	75	f	3	Alzheimer's Dementia (mild)
AZ34	74	f	18	Alzheimer's Dementia (moderate-definite)
AZ52	68	f	36	Alzheimer's Dementia (severe)
AZ53	85	f	2	Alzheimer's Dementia – (Bronchial pneumonia)
AZ57	82	m	14.5	Alzheimer's Dementia – (Bronchial pneumonia)
AZ58	75	m	20	Alzheimer's Dementia (severe)
AZ59	83	m	15	Alzheimer's Dementia – (Cardiopulm collapse, mild)
AZ72	70	f	7	Alzheimer's Dementia

Table 3: Mouse Lines reflecting aspects of AD pathology.

	APPPS1 (Radde et al. 2006)	**3xTg** (Oddo et al. 2003)	**PDAPP** (Games et al. 1995)	**Tg2576** (Hsiao et al. 1996)
Promoter	Thy1;neuronal	Thy1: Neuronal PS1: neuronal and glial (knock-in)	PDGFβ; mostly neuronal (Sasahara et al. 1991)	Hamster Prion Protein (PrP); neuronal
Start of Promoter Expression	Postnatal	Postnatal: APP, Tau Prenatal: PS1 (knock-in)	Prenatal: Aβ	From E13.5 on (Manson et al. 1992)
APP Mutation	**KM670/671NL** (Swedish double mutation)	**KM670/671NL** (Swedish double-mutation)	**V717F**	**KM670/671NL** (Swedish double mutation)
PS1 Mutation	**L166P**	**M146V**	--	--
Tau Mutation	--	**P301L**	--	--
Onset of Plaque and Tau/Tangle Pathology	**Plaques:** 2-3 months of age	**Plaques:** 6 months of age **Tangles:** 12-15 months of age	**Plaques:** 6-9 months of age	**Plaques:** 9-11 months of age
Neuronal, Synaptic phenotype	No global neuronal loss (Radde et al. 2006; Rupp et al. 2010)	Synaptic dysfunction (EPSPs) and LTP deficits present at 6 months of age (Oddo et al. 2003)	Decrease in presynaptic densities in 6-9 months old mice (Dodart et al. 2000; Larson et al. 1999)	No neuronal loss No synaptic loss (Irizarry et al. 1997)

Figure Legends

Figure 1 Focal demyelination and myelin amounts in APPPS1 mice.

(A-F) Overviews and higher magnifications (B´,E´) of myelin shown by Gallyas impregnation in the gray (A, B, D, E) and white matter (C, F) in controls (A-C) and APPPS1 (D-F) mice at 6 and 11 months of age. (G) Immunostainings of the cortical gray matter for MAG in controls and APPPS1 mice at 6 and 11 months of age. The arrowheads indicate the focal demyelination in plaque core areas. To examine total protein amounts of NF70 and CNPase, western blot analysis was performed on cerebral cortex of 6 and 9 month old animals. (H) shows a representative Western blot. (I) shows the ratio between the total pixels of CNPase divided by NF70. Ratio of controls at 6 months was set as 100%. Scale bars: 200 µm (in C, F), 100 µm (in A, B, D, E), 50 µm (B', E',G).

Figure 2 Myelin integrity in APPPS1 mice at 6 months of age.

(A-F) depict electron microscopic pictures of the cortical gray matter in control (A) or APPPS1 mice (B-F). (G-L) show the cortical white matter in wild type (G) or transgenic (H-L) animals. Examples for gray and white matter aberrations observed in APPPS1 mice like an axon surrounded by two myelin sheaths (D, J), balooned myelin (F, L) degenerated sheaths (E), excess cytoplasm in the inner loop (K), abnormal myelin outfoldings (C, I) or other myelin abnormalities (B, H) are depicted. (M) Quantification of myelin defects per number of axons. Magnifications are indicated within the pictures. Arrowheads point at aberrations.

Figure 3 Olig2+ cells in APPPS1 mice.

(A) Representative stainings for BrdU, GSTπ and Olig2 after 2 weeks BrdU application in control and APPPS1 mice at the age of 6 months. White arrowheads highlight Olig2+/BrdU+ cells, while yellow arrowheads point toward Olig2+/GSTπ+ cells. (B) Quantification of the

number of Olig2+ cells per mm^2 at different ages in APPPS1 and control animals. (C) Histogram showing the composition of Olig2+ cells at the age of 6 months. (D) Number of proliferating Olig2+ cells per mm^2 of the cortical gray matter after a 2 week BrdU pulse. Scale bars: 100 µm.

Figure 4 Increased proliferation and maturation of NG2+ cells in the cortical gray matter of APPPS1 mice.

Proliferation (A-B) and differentiation (C-D) of gray matter OPCs was investigated by different BrdU pulses. (A) Quantification of proliferating NG2+ cells after a 2 week BrdU-pulse at 6 months of age. (B) Representative immunostainings for BrdU and NG2 and merged pictures used for the quantification shown in (A). (C) Quantification of GSTπ/BrdU double-positive cells in 8 months old animals per mm^2 representing the newly generated oligodendrocytes after a 4 week BrdU retaining period. (D) Immunostainings showing examples for GSTπ+/BrdU+ cells. The white arrowheads indicate double-positive cells, while the dark arrows point at single positive cells. The inlay in (D) shows a higher magnification of a double positive cell. Scale bars: 50 µm and 20 µm for the inlay in (D).

Figure 5 Increased proliferation and maturation of NG2+ cells in the cortical white matter of APPPS1 mice.

(A) Quantification of NG2+/BrdU+ double-positive cells per mm^2 after a 2 weeks BrdU pulse in the WM of 6 months old animals. (B) Quantification of newly generated GSTπ/BrdU double-positive cells after a 4 weeks retaining period. (C-C´´) show a representative picture of a GSTπ/BrdU immunostaining, with the inlay (D-D´´) representing a higher magnification of a double-positive cell. Arrowheads point at double positive cells. Scale bars: 20µm.

Figure 6 OLIG2+ cells in human Alzheimer's disease pathology.

(A, B) Representative pictures of OLIG2+ cells in the cortical gray (A) and white (B) matter of healthy control patients and human AD patients of the sensory motor cortex. (C-H) Histograms depicting the total number of Olig2+ cells per mm^2 in the cortical gray and white matter of human control and AD patients of Sensory Motor Cortex (C, D), Superior Temporal Gyrus (E, F) and Mid Frontal Gyrus (G, H). Scale bars: 100μm.

Supplementary Figure 1 Plaque load at different ages in APPPS1 mice.

(A-C) Pictures show sagittal sections of APPPS1 mice at (A) 3, (B) 6 and (C) 9 months of age. The sections were immunostained with the 6E10 antibody, detecting human APP and Aβ. (D) Higher power images showing plaque deposition already at 3 months of age. Scale bars: 200μm.

Supplementary Figure 2 Percentage of OLIG2+ cells amongst the total amount of DAPI+ cells.

(A,C,E) indicate the percentage of OLIG2+ cells over the total number of DAPI+ cells in different cortical GM regions. (B,D,F) indicate the percentage of OLIG2+ cells over the total number of DAPI+ cells in different cortical WM regions in human Sensory Motor Cortex, Superior Temporal Gyrus and Mid Frontal Gyrus of healthy and AD tissue.

Figure 1

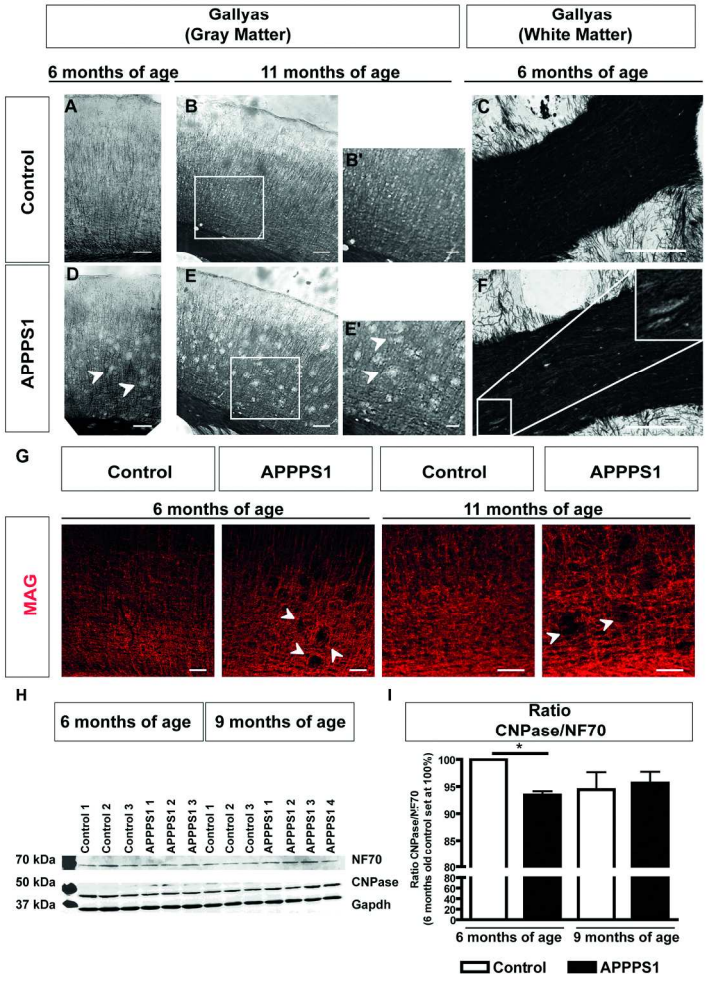

Focal demyelination and myelin amounts in APPPS1 mice.
(A-F) Overviews and higher magnifications (B´,E´) of myelin shown by Gallyas impregnation in the gray (A, B, D, E) and white matter (C, F) in controls (A-C) and APPPS1 (D-F) mice at 6 and 11 months of age. (G) Immunostainings of the cortical gray matter for MAG in controls and APPPS1 mice at 6 and 11 months of age. The arrowheads indicate the focal demyelination in plaque core areas.

180x254mm (300 x 300 DPI)

Figure 2

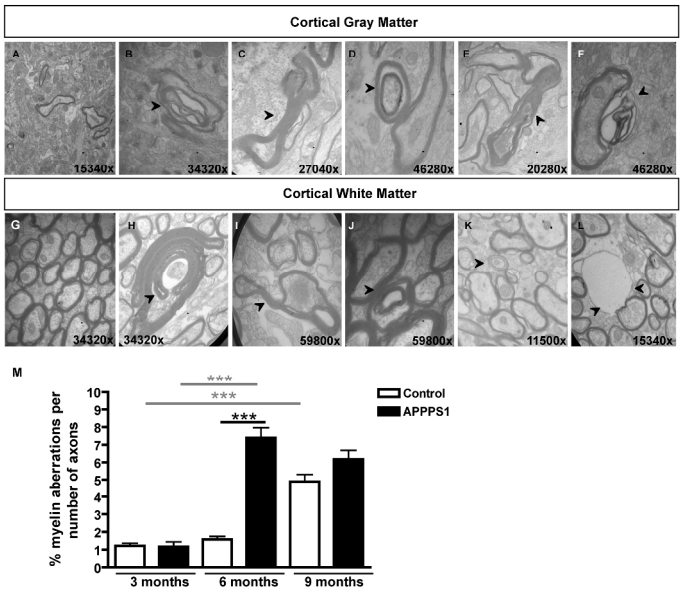

Myelin integrity in APPPS1 mice at 6 months of age.
(A-F) depict electron microscopic pictures of the cortical gray matter in control (A) or APPPS1 mice (B-F). (G-L) show the cortical white matter in wild type (G) or transgenic (H-L) animals. Examples for gray and white matter aberrations observed in APPPS1 mice like an axon surrounded by two myelin sheaths (D, J), balooned myelin (F, L) degenerated sheaths (E), excess cytoplasm in the inner loop (K), abnormal myelin outfoldings (C, I) or other myelin abnormalities (B, H) are depicted. (M) Quantification of myelin defects per number of axons. Magnifications are indicated within the pictures. Arrowheads point at aberrations.
291x186mm (300 x 300 DPI)

Figure 3

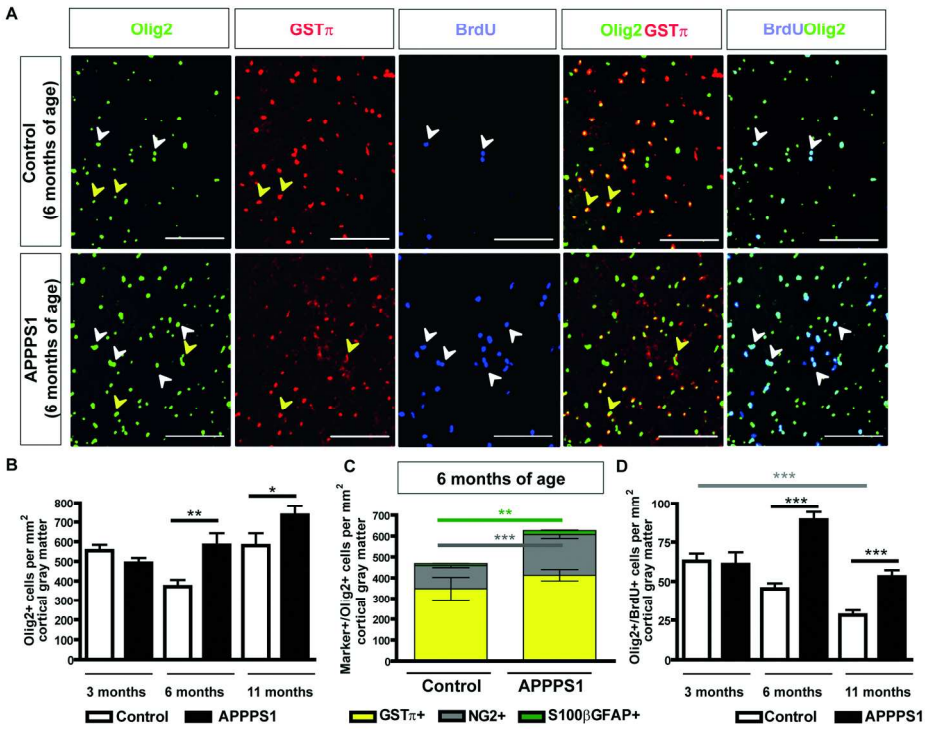

Olig2+ cells in APPPS1 mice.
(A) Representative stainings for BrdU, GSTπ and Olig2 after 2 weeks BrdU application in control and APPPS1 mice at the age of 6 months. White arrowheads highlight Olig2+/BrdU+ cells, while yellow arrowheads point toward Olig2+/GSTπ+ cells. (B) Quantification of the number of Olig2+ cells per mm^2 at different ages in APPPS1 and control animals. (C) Histogram showing the composition of Olig2+ cells at the age of 6 months. (D) Number of proliferating Olig2+ cells per mm^2 of the cortical gray matter after a 2 week BrdU pulse. Scale bars: 100 µm.
180x155mm (300 x 300 DPI)

Figure 4

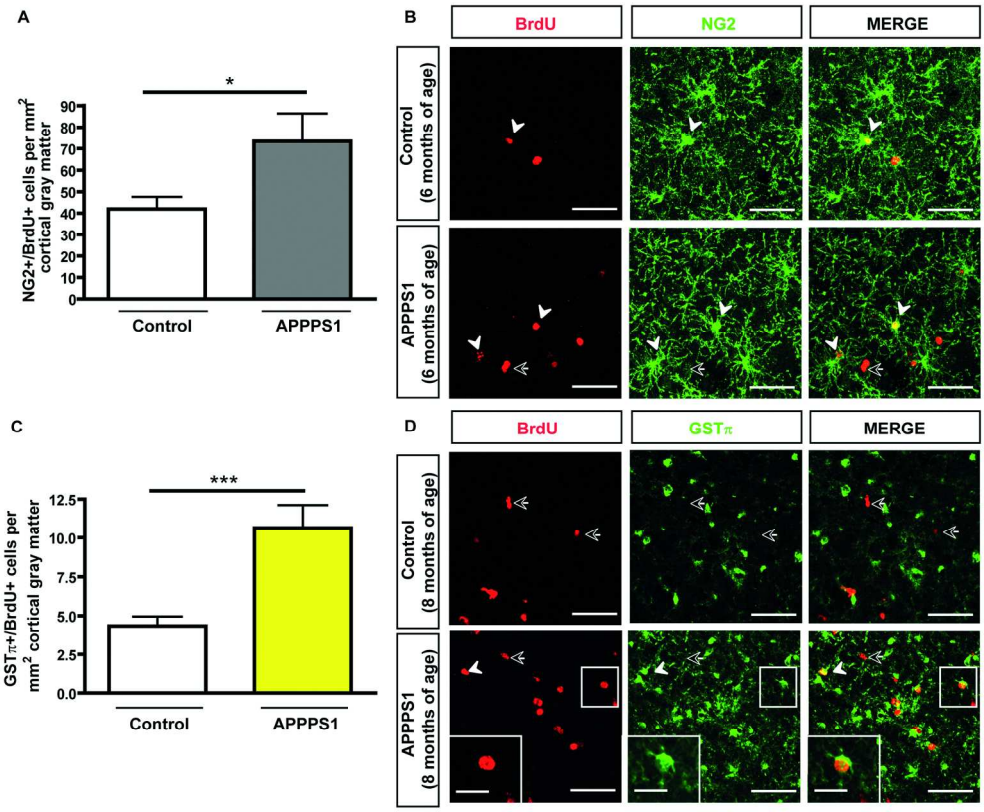

Figure 4 Increased proliferation and maturation of NG2+ cells in the cortical gray matter of APPPS1 mice. Proliferation (A-B) and differentiation (C-D) of gray matter OPCs was investigated by different BrdU pulses. (A) Quantification of proliferating NG2+ cells after a 2 week BrdU-pulse at 6 months of age. (B) Representative immunostainings for BrdU and NG2 and merged pictures used for the quantification shown in (A). (C) Quantification of GSTπ/BrdU double-positive cells in 8 months old animals per mm2 representing the newly generated oligodendrocytes after a 4 week BrdU retaining period. (D) Immunostainings showing examples for GSTπ+/BrdU+ cells. The white arrowheads indicate double-positive cells, while the dark arrows point at single positive cells. The inlay in (D) shows a higher magnification of a double positive cell. Scale bars: 50 µm and 20 µm for the inlay in (D).
180x160mm (300 x 300 DPI)

Figure 5

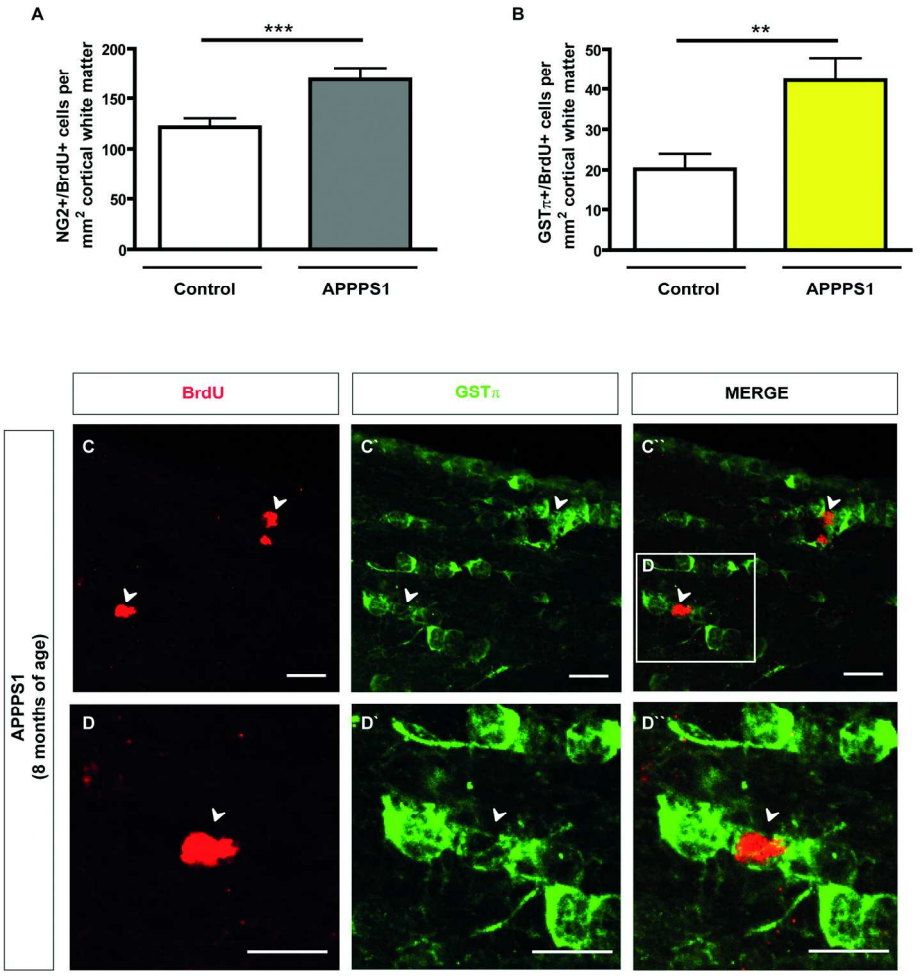

Increased proliferation and maturation of NG2+ cells in the cortical white matter of APPPS1 mice. (A) Quantification of NG2+/BrdU+ double-positive cells per mm2 after a 2 weeks BrdU pulse in the WM of 6 months old animals. (B) Quantification of newly generated GSTπ/BrdU double-positive cells after a 4 weeks retaining period. (C-C´´) show a representative picture of a GSTπ/BrdU immunostaining, with the inlay (D-D´´) representing a higher magnification of a double-positive cell. Arrowheads point at double positive cells. Scale bars: 20μm.
180x208mm (300 x 300 DPI)

Figure 6

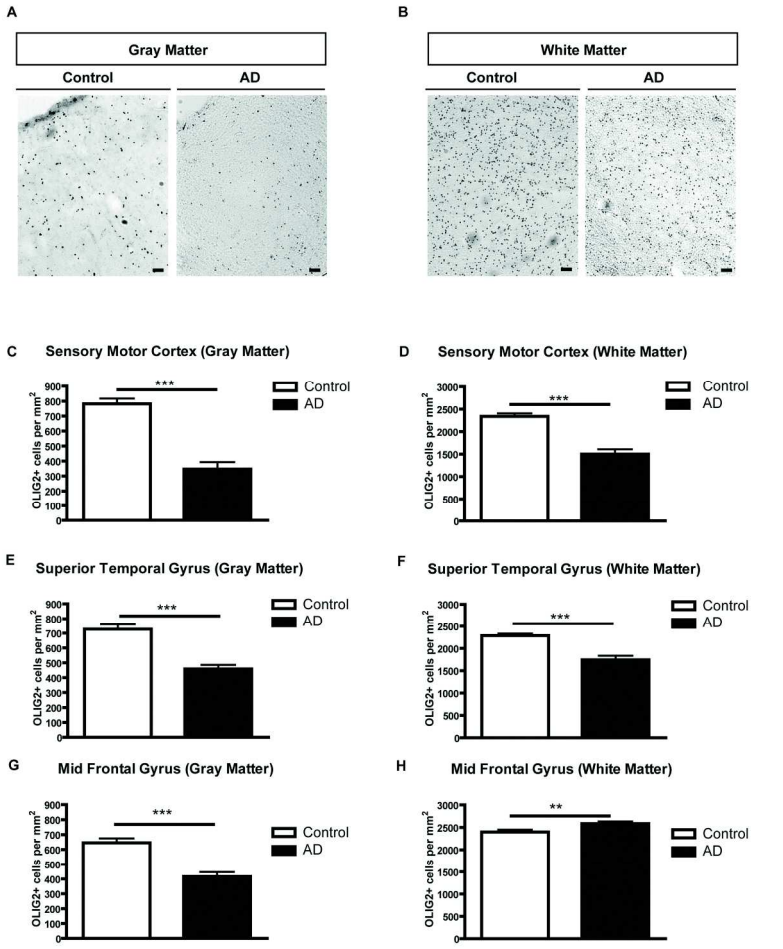

OLIG2+ cells in human Alzheimer's disease pathology.
(A, B) Representative pictures of OLIG2+ cells in the cortical gray (A) and white (B) matter of healthy control patients and human AD patients of the sensory motor cortex. (C-H) Histograms depicting the total number of Olig2+ cells per mm2 in the cortical gray and white matter of human control and AD patients of Sensory Motor Cortex (C, D), Superior Temporal Gyrus (E, F) and Mid Frontal Gyrus (G, H). Scale bars: 100μm.
180x254mm (300 x 300 DPI)

Supplementary Figure 1

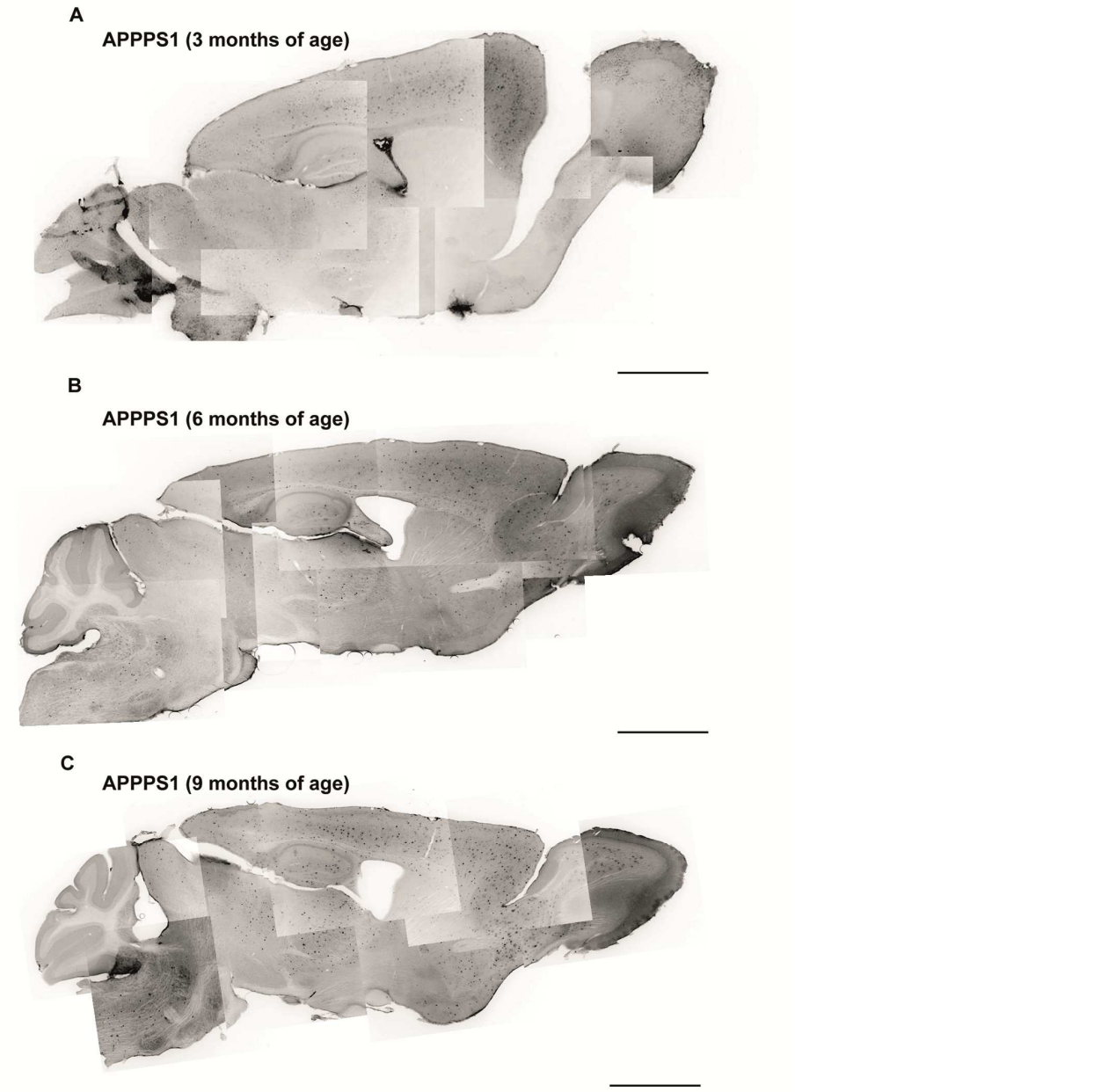

Supplementary figure 2

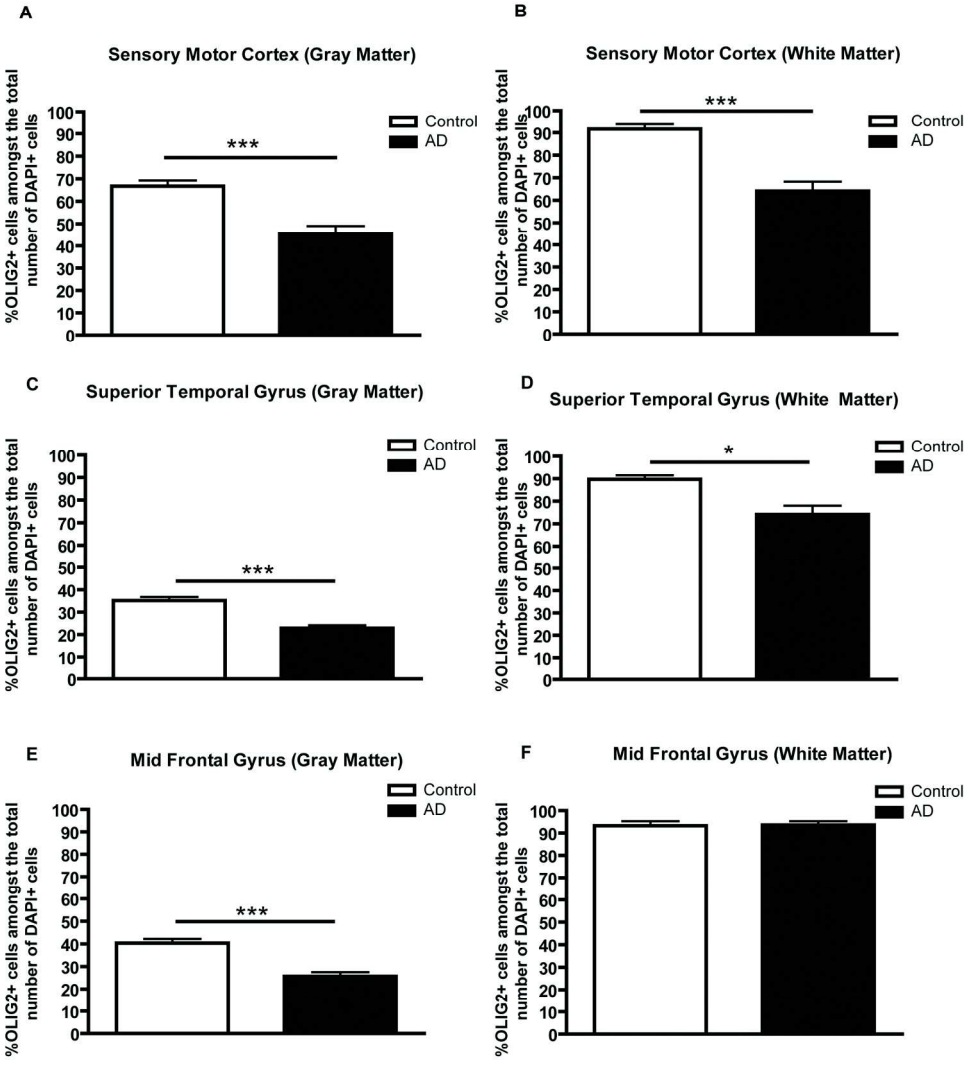

Percentage of OLIG2+ cells amongst the total amount of DAPI+ cells.
(A,C,E) indicate the percentage of OLIG2+ cells over the total number of DAPI+ cells in different cortical GM regions. (B,D,F) indicate the percentage of OLIG2+ cells over the total number of DAPI+ cells in different cortical WM regions in human Sensory Motor Cortex, Superior Temporal Gyrus and Mid Frontal Gyrus of healthy and AD tissue.
180x222mm (300 x 300 DPI)

Table 1: List of Primary Antibodies

Antibody	Host	Dilution	Company
Anti-Aβ/APP	clone 6E10, mouse	1:200	Millipore
anti-Bromodeoxyuridine (BrdU)	rat	1:200	Biozol
anti glial-fibrillary acidic protein (GFAP)	mouse	1:1000	Sigma Aldrich
anti glial-fibrillary acidic protein (GFAP)	rabbit	1:1000	DAKO
anti-Glutathione-S-transferase π (GSTπ)	mouse	1:500	BD Bioscience
anti-NG2	rabbit	1:200	Chemicon
anti-Olig2	rabbit	1:500	Chemicon
anti-S100β	mouse	1:1000	Sigma Aldrich
anti-MAG	mouse	1:100	Chemicon

Table 2: List of human Cases Used in this Study

Case	Age (years)	Sex	Postmortem delay (hours)	Indication - (Cause of death)
H123	78	f	7.5	Control – (Rupt. Aortic aneurysm)
H126	35	f	10	Control – (Suicide/hanging)
H136	75	m	13	Control – (Rupt. Aorta, abdom. Aneurysm)
H137	77	m	12	Control – (Coronary artherosclerosis)
H150	78	m	11	Control – (Rupt. Myocardial infarction)
H191	77	m	20	Control – (Ischaemic heart disease)
H192	65	f	24	Control – (Ischaemic heart disease)
H193	71	m	23	Control – (Ischaemic heart disease)
AZ32	75	f	3	Alzheimer's Dementia (mild)
AZ34	74	f	18	Alzheimer's Dementia (moderate-definite)
AZ52	68	f	36	Alzheimer's Dementia (severe)
AZ53	85	f	2	Alzheimer's Dementia – (Bronchial pneumonia)
AZ57	82	m	14.5	Alzheimer's Dementia – (Bronchial pneumonia)
AZ58	75	m	20	Alzheimer's Dementia (severe)
AZ59	83	m	15	Alzheimer's Dementia – (Cardiopulm collapse, mild)
AZ72	70	f	7	Alzheimer's Dementia

Table 3: Mouse Lines reflecting aspects of AD pathology.

	APPPS1 (Radde et al. 2006)	**3xTg** (Oddo et al. 2003)	**PDAPP** (Games et al. 1995)	**Tg2576** (Hsiao et al. 1996)
Promoter	Thy1;neuronal	Thy1: Neuronal PS1: neuronal and glial (knock-in)	PDGFβ; mostly neuronal (Sasahara et al. 1991)	Hamster Prion Protein (PrP); neuronal
Start of Promoter Expression	Postnatal	Postnatal: APP, Tau Prenatal: PS1 (knock-in)	Prenatal: Aβ	From E13.5 on (Manson et al. 1992)
APP Mutation	**KM670/671NL** (Swedish double mutation)	**KM670/671NL** (Swedish double-mutation)	**V717F**	**KM670/671NL** (Swedish double mutation)
PS1 Mutation	**L166P**	**M146V**	--	--
Tau Mutation	--	**P301L**	--	--
Onset of Plaque and Tau/Tangle Pathology	**Plaques:** 2-3 months of age	**Plaques:** 6 months of age **Tangles:** 12-15 months of age	**Plaques:** 6-9 months of age	**Plaques:** 9-11 months of age
Neuronal, Synaptic phenotype	No global neuronal loss (Radde et al. 2006; Rupp et al. 2010)	Synaptic dysfunction (EPSPs) and LTP deficits present at 6 months of age (Oddo et al. 2003)	Decrease in presynaptic densities in 6-9 months old mice (Dodart et al. 2000; Larson et al. 1999)	No neuronal loss No synaptic loss (Irizarry et al. 1997)